polymer

Automatic coarse graining of polymers

Roland Faller*

Department of Chemical Engineering and Materials Science, University of California-Davis, Davis, CA 95616, USA

Abstract

Several recently proposed semi-automatic and fully-automatic coarse-graining schemes for polymer simulations are discussed. All these techniques derive effective potentials for multi-atom units or super-atoms from atomistic simulations. These include techniques relying on single chain simulations in vacuum and self-consistent optimizations from the melt like the simplex method and the inverted Boltzmann method. The focus is on matching the polymer structure on different scales. Several ways to obtain a time-scale for dynamic mapping are discussed additionally. Finally, similarities to other simulation areas where automatic optimization are applied as well are pointed out.
© 2004 Elsevier Ltd. All rights reserved.

Keywords: Polymer simulations; Multi-scale techniques

1. Introduction

Polymers with their large variety of important length scales pose a formidable challenge for computer simulations. Over the last decades various techniques to handle the problems on the different length scales separately have been developed. Especially simulations in full atomistic detail [1–5], and with one interaction center for each monomer [6–8] or for each polymer [9] have gained a lot of attention.

More recently, it has been realized that a connection between the arising length and time scales are necessary. To this end, a number of coarse-graining techniques have been devised [10–20] where simulations on more than one length scale are combined in order to get a better understanding of the system as a whole. It has even been proposed that simulations on both scales can be performed in one single simulation box [11,20]. The purpose of this contribution is to critically analyze several of the most recent automatic mapping schemes for coarse-graining in polymer research. This comprises a technique combining atomistic single chain Monte Carlo with molecular dynamics on the meso-scale [10], the automatic simplex mapping technique [21,22], and a number of physically inspired techniques [13,17,18]. All these techniques have been implemented in

automatized schemes which in principle allow to obtain a coarse-grained polymer model on the meso-scale without human intervention if the atomistic simulations have been performed. Based on the atomistic simulations a target function has to be defined and optimized against in the meso-scale simulation.

Techniques which either rely on the use of lattice simulations or which cannot be implemented in an automatic manner have been left out on purpose in this contribution. The reader is referred to other reviews including such techniques [12,16,19].

There are many reasons for applying coarse-graining schemes for polymer simulations. The overall structure of a polymer in melt or solution often shall be reproduced faithfully except for the local atomistic detail. This improves the speed and memory requirements of the simulation and by that allow larger simulations or longer chains. Simulations of long chains are necessary but the experimentally relevant chain lengths cannot be reached by atomistically detailed simulations. Even if computer speed increases in the future as it did over the last decades, we are still decades away from doing simulations of chains with thousands monomers in a fully atomistically detailed simulated melt. The relevant relaxation times increase by an exponent of $N^{3.4}$ with chain length N for large chains [23]. And, even if it were possible to perform such simulations their usefulness would be questionable as the vast amount of data would be very difficult to analyze as the

* Tel.: +1-530-752-5839; fax: +1-530-752-1031.
  E-mail address: rfaller@ucdavis.edu (R. Faller).

interesting observables would be difficult to filter out. A lot of questions on large scales have been answered by simple bead-spring models. These models are able to get interesting scaling behaviors and by this a lot of basic understanding. In order to get compare directly to experiments, however, one needs a meso-scale model which does not represent generically 'a polymer' but has an identity of a specific polymer. To this end, a combination of atomistic and meso-scale models which can be mapped uniquely onto each other is necessary. In this case issues appearing on different length scales can be answered consistently.

The remainder of this article is organized as follows. Section 2 deals with the various possibilities of static mapping, Section 3 with dynamic mapping which has gained much less attention and in the end conclusions will be drawn and connections to other automatic optimization techniques in molecular simulation will be shown.

2. Static mapping

2.1. The concept of super-atoms

The methods to be discussed here deal all with two length scales. Most often these are the atomistic scale and the meso-scale. However, for the methods to work this is not necessary. For the remainder of this contribution an atomistic simulation is defined to be a simulation where all atoms are present or only the hydrogens are neglected. The latter is often called a united atom model. A meso-scale model is defined to be a model where a group of atoms is replaced by one interaction center. This group is typically of the size of a monomer. We call such a unit a super-atom.

Thus, a part of a polymer chain comprising a few atoms (typically $10-30$) will be represented by one interaction center. The super-atoms are the only interaction centers in the meso-scale simulation. The interaction between super-atoms has to implicitly carry the information of the interactions between the atoms in their local geometrical arrangements imposed by the bonding. Fig. 1 shows some typical examples of super atom representation of polymers.

The choice of super-atoms is arbitrary in principal. But there are a number of criteria which have been established. It is very effective if the distance between super-atoms along the chain is relatively rigidly defined as in that case the bonding potential is just a harmonic bond [18]. Fig. 2 shows this using *cis*-1-4-poly-isoprene. The obvious choice of the center of mass of the double bond leads to a doubly peaked bond distribution whereas the choice of the super-atom center being placed between atomistic monomers results in a clear single peak. Such a distribution can easily be modeled by a single Gaussian which is produced by a harmonic bond potential The height to width ratio of the Gaussian peak defines the harmonic bond strength. The underlying reason for the two strongly different distributions is that the double bond is very rigid and does not allow any
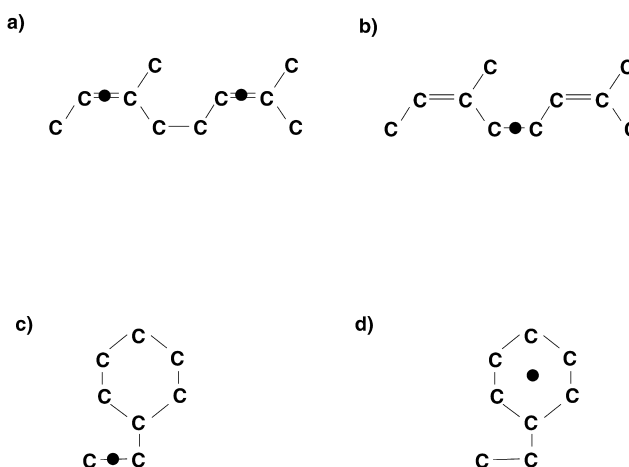

Fig. 1. Illustration of super-atoms representing polymers. The hydrogens are left out for clarity. (a) *Cis*-polyisoprene physical monomer, center of the super atom in the middle of the double bond; (b) polyisoprene pseudomonomer, center of the super atom between two physical monomers; (c) polystyrene, super-atom center on the single bond in the monomer; (d) polystyrene, super-atom center in the center of the ring. All the super-atom centers are marked by black dots.
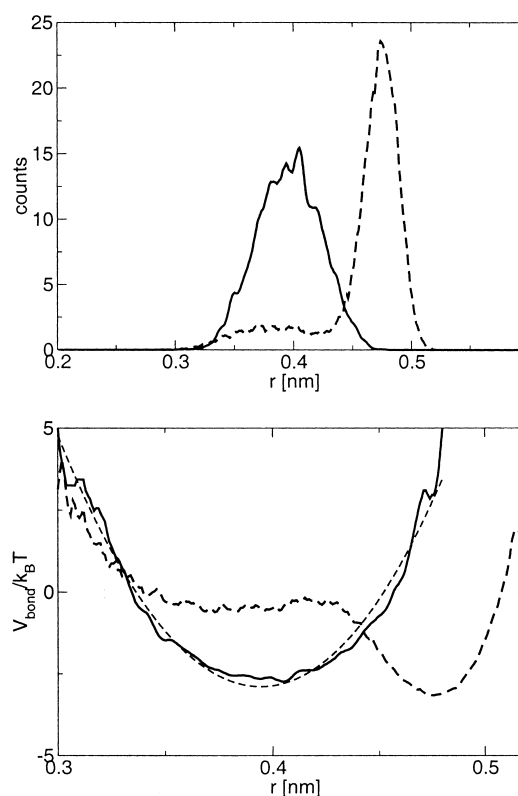

Fig. 2. Left: bond length distributions arising from the possible choices of super-atoms in *cis*-polyisoprene of Fig. 1. The single peaked solid line corresponds to the center of the super-atom on the single bond between atomistic monomers (Fig. 1(b)), the dashed line to the super-atom in the center of the double bond (Fig. 1(a)). All histograms are normalized that the integral equals 1. Right: bond potentials gained by direct Boltzmann inversion of the distributions of the left hand side (same line styles). The thin broken line is a harmonic fit to the pseudomonomer potential. Curves were locally smoothed for differentiability.

torsional degrees of freedom whereas the single bonds can easily flip from one torsional state to another. As the centers of mass of the double bond are effectively connected by single bonds and vice versa the double bonds lead to the sharply peaked distribution and the different torsion states of the single bonds lead to more than one peak making it more difficult to model the distribution by a simple bond potential. Additionally the multiplicity of peaks would lead to an interdependence of bond and angle potentials.

Moreover, it is advantageous to have the space occupied by the atoms represented in one super-atom being spherical in order to avoid anisotropic potentials. Almost all schemes use a spherical potential to model the space occupied by the super-atom [10,11,13,18,21]. This occupied space can in the first approximation be viewed as the elliptic hull of the atoms. Generalizations to anisotropic potentials have been attempted [24]. The offset by the much higher complexity of the simulation can in most cases not been overcome by the only slightly higher accuracy.

If a single spherical potential is not satisfactory as, e.g. for diphenylcarbonate [21] or polycarbonates [10] it is more economical to use more than one spherical super-atom per monomer than a non-spherical one. Abrams et al. showed that in the case of polycarbonate one needs 5 spherical interaction center per atomistic monomer in order to get a good representation of the underlying polymer [25] whereas 3 anisotropic beads have been used by Hahn et al. [24].

2.2. Single chain distribution potentials

Tschöp et al. proposed a technique for mapping the structure of a polymer to a model containing much less interaction sites [10]. The model starts out with a detailed quantum chemical calculation of short segments of the polymer chain in order to obtain an accurate torsion potential. This quantum chemically determined distributions are then used to perform single chain Monte Carlo simulations in vacuum. The corresponding distributions of super-atoms are recorded. The recorded distributions are bond lengths, bond angles and torsions. In order to accurately gain a potential out of these distributions they have to be weighted by the corresponding Jacobians. For example, for the bond lengths the Jacobian is just r^2 which stems from the transformation from spherical to Cartesian coordinates. Then they are Boltzmann-inverted to obtain intra-molecular potentials between super atoms, i.e. a potential is derived from the distribution. Formally, the Boltzmann inversion leads to a free energy difference but in vacuum this equals the potential energy. This difference will become crucial in the following sections.

$$V(\zeta) = -k_{\mathrm{B}}T \ln p(\zeta) \qquad (1)$$

here, ζ can stand for bond lengths, bond angles and torsions alike. The distribution $p(\zeta)$ is taken after the Jacobian correction. In this way, a complete set of intra-molecular potentials has been obtained. It is noteworthy that this potential is completely numerical. In order to be able to calculate a derivative to obtain the forces local splines or similar techniques can be used to smooth it. Cross dependencies of the different potentials (e.g. bond and angle) are neglected for computational reasons. As explained above they can be eliminated by the proper choice of mapping points.

In the original work, this elaborate intra-molecular potential was combined with a simple repulsive Lennard–Jones or WCA potential [26] to reproduce the density.

$$V_{\mathrm{WCA}} = 4\epsilon\left[\left(\frac{\sigma}{r}\right)^{12} - \left(\frac{\sigma}{r}\right)^{6}\right] \quad r < \sqrt[2\sigma]{6} \qquad (2)$$

here, σ is the interaction radius (size) of the monomer, ϵ is the interaction strength, and r is the distance between corresponding monomers.

This method was successful in calculating the structure factor of polycarbonates [27]. A similar approach has been applied to a simple hydrocarbon chain where the super-atom center is taken as the center of mass of n monomers [15]. In this case, the starting point was an atomistic molecular dynamics simulation. For the non-bonded potential also a potential of mean force approach has been taken. So the radial distribution function of two dilute polymers is used to determine the non-bonded potential. For small molecules, this can be used directly [11]. For polymers at small distances, the connectivity leads to a severe restriction on the possible conformations so a restricted pair distribution function taking connectivity into account has to be used. This approach does not separate the simulations of the atomistic and the coarse-grained models and bases on the reversible work theorem [11,20]

$$e^{-\beta W(r)} = \frac{\sum\limits_{i} e^{-\beta U_i(r)}}{\sum\limits_{i} e^{-\beta U_i(\infty)}} \qquad (3)$$

where W is the reversible work and this can be used as a potential to obtain the same structure as the atomistic model. The appearance of the inverse temperature $\beta = (k_{\mathrm{B}}T)^{-1}$ scaled by the Boltzmann factor k_{B} makes it clear that this is valid only at the specified temperature. The potential U is the full potential energy of the system with the two sites under focus fixed at a distance r apart. Fully detailed and mesoscopically modeled particles coexist in the very same simulation. The detailed particles carry two potentials as they interact with the non-detailed particles as if they were non-detailed particles (cf. Fig. 3). Actually, the two types of particles can even be bonded to each other in order to get the correct potential along a polymer chain as pointed out in Ref. [15] where also the automatic implementation was shown.
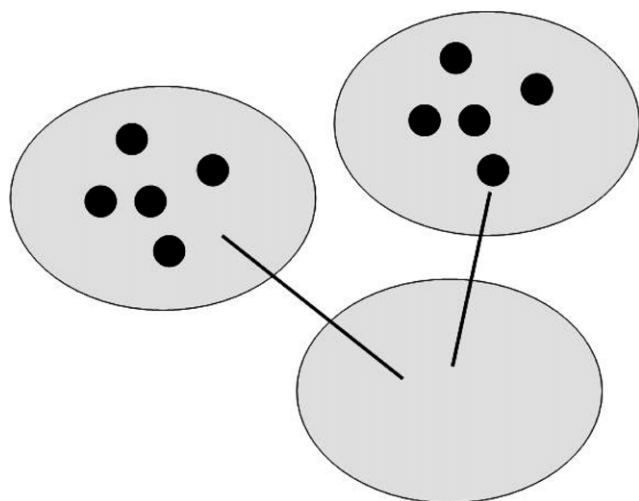
Fig. 3. The scheme of McCoy et al. uses different degrees of detail in the very same simulation. The figure shows two particles which exist on both scales. These interact by their atomistic potentials. The atomistically detailed interact with the purely mesoscopic by the mesoscopic potential as do the purely mesoscopic among themselves. Some of the particles are bonded to form a polymer.

2.3. Simplex

Recently, more direct ways of linking atomistic melt simulations and meso-scale melt simulations have been developed. The idea is to systematically and self-consistently reproduce structure and thermodynamics of the atomistic simulation on the meso-scale. As this is an optimization problem mathematical optimization techniques can be applied directly. One of the most robust although not very efficient multi-dimensional optimizers is the simplex [28]. It has the advantage that it does not rely on any derivatives, as they are very difficult to obtain in the simulation. The simplex was first applied to optimizing atomistic simulation models to experimental data [29]. The idea is to view the experimental observables, e.g. the density ρ, as a function f of the parameters of the simulation model B_i, e.g. the Lennard–Jones parameters

$$\rho = f(\{B_i\}) \tag{4}$$

this function in multi-dimensional space is now optimized by the simplex technique. In order for the simplex to be applicable a single valued function with a minimum at the target has to be defined. This is easily accomplished by the sum of square deviations from target values

$$f = \sum_i [A(\{\epsilon_i\}, \{\sigma_i\}) - A_{\text{target}}]^2 \tag{5}$$

here, A represents any thermodynamic observable to be reproduced in this scheme with a target value A_{target}; $\{\epsilon_i\}$, $\{\sigma_i\}$ are the full set of Lennard–Jones parameters. Every function evaluation includes a complete equilibration sequence for the given parameters, a production run and the analysis. In order to ensure equilibration, it was made certain that no drift in the observables remained and an

automatic detection of equilibration was developed [29]. Very recently, it has been shown that the derivatives of the observables with respect to the parameters of the simulation model can also be calculated and therefore more efficient optimizers can be used [30].

In the context of polymer mapping, the target functions are not experimental observables but the structure of the system. So radial distribution functions are the aim of the technique. To this end one views any point of the radial distribution function $g(R)$ in the interval $[R_i, R_i + 1]$ as a different observable which is to be reproduced. The function to be minimized is the integral over the squared difference in radial distribution functions [21]. If necessary, a weighting function can additionally be introduced [18,21]. An exponential decay is a good choice as the local structure around the first peak in the rdf is most crucial and most difficult to reproduce.

$$f = \int \mathrm{d}r w(r)[g(r) - g_{\text{target}}(r)]^2 \tag{6}$$

A drawback of the simplex technique is that it cannot use numerical potentials as a relatively small set of parameters defining the parameter space is needed. The limit is typically 4–6 independent parameters B_i. An increase in dimensionality of this space increases the need for computational resources tremendously. A good choice for such parameters are a Lennard–Jones like expansion [21,22]

$$V(R) = \sum_i \frac{B_i}{r^i} \tag{7}$$

where i has been used to span the even numbers from 6 to 12. This technique has been successful to reproduce monomers of polyisoprene [21]. The structure of small molecules like diphenylcarbonate could be described by this technique as well [21]. The application to polymers showed some deficiencies [22] which led to the development of better suited algorithms.

2.4. Physically inspired optimization methods

The iterative Boltzmann method was developed in order to circumvent the problems encountered with the simplex technique [17,18]. It is an optimization aiming at the structure of an atomistic simulation. It showed its strength by being able to reproduce the structure of trans-1,4-polyisoprene where the simplex technique failed [17,18]. The idea is to use a physically inspired optimization technique to speed up the convergence and at the same time get rid of the limitation on the number of parameters as imposed by the simplex technique.

As discussed above, in the limit of infinite dilution one could use the potential of mean force gained by Boltzmann inverting the pair distribution function to get an interaction potential between monomers, this would be the non-bonded generalization of the above described single chain approach.

Similar ideas have been used to calculate potentials of mean force (PMF) of large particles like colloids in matrices of small particles where the small particles play only the role of a homogeneous background [31,32]. In concentrated solutions or melts, the structure is defined by an interplay of the PMF and the packing of atoms or monomers. It has been shown that simple packing arguments can account for the largest part of local orientation correlations in dense melts [33]. Thus, a direct calculation of the potential of mean force is not correct. Still the use of the PMF idea as a way to iteratively approach the correct potential is possible and is used by the iterative Boltzmann method. A melt or solution of polymers is simulated in atomistic detail to obtain a pair distribution function. For every iteration a one-to-one correspondence between the effects at a distance r_0 and the potential $V(r_0)$ (or force $-\mathrm{d}_r V(r)|_{r=r_0}$) at the same distance r is assumed. However, this is not a limitation as the iterative procedure takes care of any other dependencies.

It becomes immediately clear from this approach that the resulting potential is numerical, as every single bin of the potential as a function of distance is optimized independently. It is possible and advantageous to enforce continuity by using weighted local averages. This is important if the function to be optimized against is relatively noisy, however, the correct way to lower the noise level is a longer atomistic simulation which of course can be prohibitive. Fig. 4 shows the different stages of a iterative Boltzmann procedure. In the beginning, a starting potential V_{start} has to be guessed. Either we take the result from a similar problem or we start with the potential of mean force by Boltzmann inversion of the target function. After this initial potential is simulated, the radial distribution function is obtained and the difference between this function and the target is determined. This leads to a correction potential which is the difference in free energy

$$\Delta V(r) = -k_{\text{B}} T \ln\left(\frac{g(r)}{g_{\text{target}}(r)} \right) \qquad (8)$$

this correction potential is added and the iteration resumes until the difference in g is deemed satisfactory. For polyisoprene 4 iterations were necessary [17]. The final result is shown at the bottom of Fig. 4.

Two alternatives to the iterative Boltzmann technique which also rely on a physically inspired optimization of the system have been proposed by Akkermans [13,14]. The degrees of freedom of the polymer under study are separated into degrees of freedom of 'blobs' and the 'bath'. The blobs play the role of the super-atoms, the bath are all other degrees of freedom which have to be integrated out. Only the super-atoms are taken into account. The target radial distribution function is expanded in a basis set with the pre-factors left for optimization

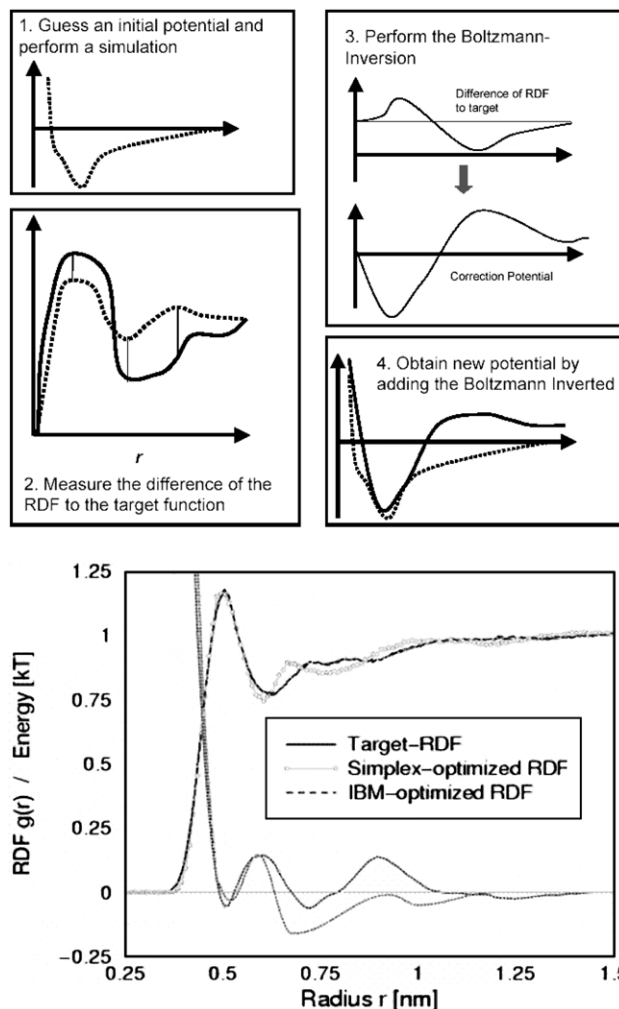$$g_{\text{target}} = \sum_i \lambda_i u_i(r) \qquad (9)$$

Fig. 4. Top: schematic explanation of the iterative Boltzmann procedure. On the lower left hand side (step 2) different stages of the potential are shown, on the upper right hand side (step 3) the corresponding radial distribution functions are depicted. Note that these sketches are for illustrative purposes only in order to emphasize the influence of the iteration. Final radial distribution functions and potentials for polyisoprene [17,18] are shown in the bottom part of the figure. The target function (solid line) and the one gained by the iterative Boltzmann method (marked IBM-optimized, dashed line) are indistinguishable. For comparison a simplex optimized structure (open circles) is shown. The resulting potentials are in the lower part of that subfigure.

The set of parameters λ can now be viewed as dynamical parameters and assigned a virtual mass $m(\lambda)$ and a velocity. So, one takes the route of an extended ensemble which is well known in molecular dynamics of constant pressure and temperature [34–36]. A Lagrangian including the λ parameters is used and the simulation proceeds using this extended Lagrangian

$$L = K(\vec{V}) + K_\lambda(\vec{v}_\lambda - U(\vec{R}, \lambda) - \Phi_\lambda(\lambda) \qquad (10)$$

where the K stands for the kinetic energies and U and Φ are the respective potentials. Akkermans et al. showed the feasibility of this technique by re-optimizing a Lennard–Jones potential. As the dynamics of the λ parameters turns

out to be problematic the same approach without the velocities can been used in a Monte Carlo procedure.

A caveat is in order here. As all the techniques described up to now only aim at the structure of the polymeric system it is not guaranteed that the thermodynamic state is correctly described. This has been pointed out by a number of researchers [13,17,37]. In order to avoid such problems, an inclusion of thermodynamic properties in the optimization scheme is necessary. For the pressure in the case of the inverted Boltzmann technique such a generalization is possible and works as follows [17]. After optimizing the structure, an additional pressure correction (pc) potential of the form

$$\Delta V_{pc}(r) = A_{pc}\left(1 - \frac{r}{r_{cut}}\right) \qquad (11)$$

is added, where A is negative if the pressure is too high and positive if it is too low. The rationale behind this choice is to have a constant force in addition to the force from the structural potential which leads to a constant shift in pressure. With such an additional potential the radial distribution function does not deteriorate strongly and a re-optimization is possible. Reith et al. showed that indeed this pressure correction solved their initial problem of an unphysically high pressure [17].

3. Dynamic mapping

Simulations in atomistic detail regularly utilize a time-step of 1 femtosecond. This time-step has to be about an order of magnitude shorter than the fastest characteristic time of the system. As customarily the bond lengths are fixed using techniques like Shake [38,39] or Rattle [35,40] the fastest time-scales in atomistic molecular dynamics are bond angle vibrations on the order of tens of femtoseconds. With a reasonable use of computer resources one can then reach into the nano-second time-range. This is long enough to compare to segmental dynamics in NMR experiments [5,41] but not long enough to compare to large time-scale experiments.

The techniques to map the statics of polymers which have been described above lead inherently to larger time-scales as the fastest inherent degrees of freedom are now motions of super-atoms of the size of monomers. If dynamic investigations are desired one has to find a correct mapping of the time-scales of the atomistic simulation to the meso-scale. Otherwise dynamic experimental comparisons are impossible.

3.1. Mapping by chain diffusion

An obvious candidate for calibrating the time-scale is the chain diffusion coefficient. At large enough times any polymer chain in a melt will end up in diffusive motion as soon as all internal degrees of freedom are relaxed. This

diffusion can be used to determine the time-scale as long as an independent mapping of the length scale is achieved. The static mapping determines the length scale; an obvious choice is the size of the monomer or the distance between super-atoms along the chain to obtain a length scale for the coarse-grained simulation [42]. If both simulations the atomistic and the coarse grained can be fully equilibrated in the sense that free diffusion of the whole chain is observed, the two diffusion coefficients can be equated and the time-scale is fixed. In most cases, a full free diffusion of the atomistic chain cannot be reached in reasonable computer time. This is especially the case when the coarse-grained simulation should be used as a means to efficiently equilibrate the structure from which atomistic simulations will be started.

Nonetheless this technique can be successful. In the case of 10-mers of polyisoprene at 413 K a dynamic mapping between a fully atomistic and a very simple coarse grained model is possible [5,42]. Only chain stiffness was used to perform the mapping. The local chain reorientation in both simulations was the same after the time-scales had been determined by the diffusion coefficient. However, the decay times of the Rouse modes were not equal which showed that the mapping by stiffness alone was too simplistic.

3.2. Mapping through segmental correlation times or Rouse model

It is often easier to use shorter, local, time scales to map the atomistic to the coarse-grained length scale. This allows a mapping also if the atomistic simulation cannot be simulated into free diffusion. Even if free diffusion can be reached, the statistical uncertainty of large time scales is often so large that a shorter time scale is a better choice for the mapping. Candidates for shorter time-scales are decay times of higher Rouse modes. Even if the Rouse model is not a perfect description of the system under study such a mapping remains meaningful. In that case this time still corresponds to a well defined relaxation time of a chain segment.

If such a chain segment consists in the extreme case of only one monomer, we end up with the segmental relaxation time or equivalently the reorientation on the monomer scale. This time-scale is very useful for dynamic mapping as it can be compared the time-scales in NMR experiments [43].

3.3. Direct mapping of the Lennard–Jones time

A completely different idea which is independent of the atomistic simulation is the mapping of the Lennard–Jones time to real time. If one applies the standard Lennard–Jones units where we measure lengths in σ, the particle diameter, energies in ϵ the depth of the Lennard–Jones potential, and masses in m the monomer mass, naturally a timescale appears which is conventionally called the Lennard–Jones

time [35,36]:

$$\tau = \sigma \sqrt{\frac{m}{\epsilon}} \qquad (12)$$

this time-scale can be used to perform the mapping to the real time-scale [18,44].

Using the polyisoprene models of Ref. [5] (atomistic at $T = 413$ K) and Ref. [17,18] (meso-scale) we get the following differences in the center-of-mass diffusion coefficient for a atomistic 10-mer: The Lennard–Jones time leads to $D_{com} = 16 \times 10^{-6}$ cm^2/s [18]. If we map the diffusion coefficient directly D is obviously the atomistic result of $D = 4.24 \times 10^{-6}$ cm^2/s. This result was actually obtained by matching the center-of-mass motion of two different models and fitting the large-scale motion of the coarser model. This was necessary as even at 413 K the simulation does not move the atomistic 10-mers into free diffusion [5]. Recently, for *cis*-polyisoprene a united atom model could be brought into free diffusion [43]. In this case, results for 8-mers ($D = 14 \times 10^{-6}$ cm^2/s) have been reported which are close to the results for the different *trans*-PI-models. This indicates that the different mappings are not far from each other but a uncertainty of the order of 2–5 has to be taken into account. For polyisoprene, this mapping actually gives a reasonable description of the experimental diffusion coefficient [43].

4. Automatic optimization—in coarse graining and elsewhere

Polymer coarse-graining is by no means the only or even the first area of computer simulations where automatic optimization techniques are applied. Already in the 70s, Torrie and Valleau [45,46] proposed a Monte Carlo technique to simplify simulations in complex energy landscapes which can easily be implemented fully automatically [47–49]. This so-called umbrella sampling bases on the idea that any bias in a Monte Carlo simulation can be used as long as it is taken into account in the analysis. For sampling reasons a uniform coverage of the interesting energy area is of advantage as in that case the system does not get trapped in any configuration but samples the whole configuration space readily. Umbrella sampling has been recently combined with parallel tempering to get a fully automatic multicanonical parallel tempering scheme [50]. An idea similar in spirit to umbrella sampling is density of states Monte Carlo which even in its very first implementation [51,52] was a completely automatic procedure. It abandons the detailed balance criterion of Monte Carlo in its early stages of sampling in order to get a better automatic optimization. This technique has since been generalized and improved in a number of ways [32,53–58]. All have in common that they aim at an automatic calculation of the free energy and in that sense the iterative Boltzmann method discussed above is only a special case of this much broader

class of techniques. It may be worthwhile to think about method transfer between the Monte Carlo calculations of the partition function as aimed by umbrella sampling or density of states Monte Carlo and polymer coarse graining.

Conclusively, one can say that the recent efforts in automatic polymer coarse-graining have led to a number of very efficient and systematic techniques to map atomistic models onto meso-scale models. Especially, the thermo-dynamically inspired iterative Boltzmann technique is fast and reliable for a number of systems. The main drawback is still the dependence on the single state point. In the transition from the atomistic to the coarse-grained scale, we gain a lot of efficiency but loose the generality of the atomistic model as the coarse-grained model is optimized to the atomistic simulation at a defined state point. Especially, in an effort to generalize the coarse graining to polymer mixtures this problem becomes apparent [59].

The state of the art in dynamic mapping is much less clear than the structural optimization. As the optimized force-fields up to now aim exclusively at the structural or thermodynamic properties, the dynamic mapping is an ad hoc step which may or may not be successful. This is especially true if solutions are to be mapped as the idea of coarse-graining is to get rid of the solvent. However, the solvent has a marked effect on the dynamics which in the coarser simulations without solvent is not present. To overcome this problem and include the dynamic effects of the solvent without explicit solvent lattice-Boltzmann simulations may be the way to go [60]. In the case of melt simulations, the solvent effects are not the problem but the resulting force-fields are up to now not able to get all the characteristic times correct at the same time so that a lot of work remains to be done.

Acknowledgements

References

[1] Paul W, Yoon DY, Smith GD. J Chem Phys 1995;103(4):1702.
[2] Moe NE, Ediger MD. Macromolecules 1996;29(16):5484.
[3] Müller-Plathe F. Chem Phys Lett 1996;252(5–6):419.
[4] Antoniadis SJ, Samara CT, Theodorou DN. Macromolecules 1998; 31(22):7944.
[5] Faller R, Müller-Plathe F, Doxastakis M, Theodorou D. Macromolecules 2001;34(5):1436.
[6] Grest GS, Kremer K. Phys Rev A 1986;33(5):R3628.
[7] Kremer K, Grest GS. J Chem Phys 1990;92(8):5057.
[8] Faller R, Müller-Plathe F, Heuer A. Macromolecules 2000;33(17): 6602.

[9] Murat M, Kremer K. J Chem Phys 1998;108(10):4340.

[10] Tschöp W, Kremer K, Batoulis J, Bürger T, Hahn O. Acta Polym 1998;49(2–3):61.

[11] McCoy JD, Curro JG. Macromolecules 1998;31(26):9362.

[12] Baschnagel J, Binder K, Doruker P, Gusev AA, Hahn O, Kremer K, Mattice WL, Müller-Plathe F, Murat M, Paul W, Santos S, Suter UW, Tries V. Adv Polym Sci 2000;152:41.

[13] Akkermans RLC, Briels WJ. J Chem Phys 2001;114(2):1020.

[14] Akkermans RLC. A structure-based coarse-grained model for polymer melts. PhD Thesis, University of Twente; 2000.

[15] Fukunaga H, Takimoto J, Doi M. J Chem Phys 2002;116(18):8183.

[16] Müller-Plathe F. Chem Phys Chem 2002;3(9):754.

[17] Reith D, Pütz M, Müller-Plathe F. J Comput Chem 2003;24(13):1624.

[18] Faller R, Reith D. Macromolecules 2003;36(14):5406.

[19] Müller-Plathe F. Soft Mater 2003;1(1):1.

[20] Tsige M, Curro JG, Grest GS, McCoy JD. Macromolecules 2003; 36(6):2158.

[21] Meyer H, Biermann O, Faller R, Reith D, Müller-Plathe F. J Chem Phys 2000;113(15):6264.

[22] Reith D, Meyer H, Müller-Plathe F. Macromolecules 2001;34(7): 2335.

[23] Strobl G. The physics of polymers, 2nd ed. Berlin: Springer; 1997.

[24] Hahn O, Delle Site L, Kremer K. Macromol Theory Simul 2001; 10(4):288.

[25] Abrams CF, Kremer K. Macromolecules 2003;36(1):260.

[26] Weeks JD, Chandler D, Andersen HC. J Chem Phys 1971;54(12): 5237.

[27] Eilhard J, Zirkel A, Tschöp W, Hahn O, Kremer K, Schärpf O, Richter D, Buchenau U. J Chem Phys 1999;110(3):1819.

[28] Press WH, Teukolsky SA, Vetterling WT, Flannery BP. Numerical recipes in C: the art of scientific computing, 2nd ed. New York: Cambridge University Press; 1992.

[29] Faller R, Schmitz H, Biermann O, Müller-Plathe F. J Comput Chem 1999;20(10):1009.

[30] Bourasseau E, Haboudou M, Boutin A, Fuchs AH, Ungerer P. J Chem Phys 2003;118(7):3020.

[31] Engkvist O, Karlström G. Chem Phys 1996;213(1–3):63.

[32] Kim EB, Faller R, Yan Q, Abbott NL, de Pablo JJ. J Chem Phys 2002; 117(16):7781.

[33] Müller-Plathe F, Schmitz H, Faller R. Prog Theory Phys Kyoto Supplements 2000;138:311.

[34] Andersen HC. J Chem Phys 1980;72(4):2384.

[35] Allen MP, Tildesley DJ. Computer simulation of liquids. Oxford: Clarendon Press; 1987.

[36] Frenkel D, Smit B. Understanding molecular simulation: from basic algorithms to applications. San Diego, CA: Academic Press; 1996.

[37] Briels WJ, Akkermans RLC. Mol Simul 2002;28(1–2):145.

[38] Ryckaert J-P, Cicotti G, Berendsen HJC. J Comput Phys 1977;23(3): 327.

[39] Müller-Plathe F, Brown D. Comput Phys Commun 1991;64(1):7.

[40] Andersen HC. J Comput Phys 1983;72(1):2384.

[41] Budzien J, Raphael C, Ediger MD, de Pablo JJ. J Chem Phys 2002; 116(18):8209.

[42] Faller R, Müller-Plathe F. Polymer 2002;43(2):621.

[43] Doxastakis M, Theodorou DN, Fytas G, Kremer F, Faller R, Müller-Plathe F, Hadjichristidis N. J Chem Phys 2003;119(13):6883.

[44] Reith D. Neue Methoden zur Computersimulation von Polymersystemen auf verschiedenen Längenskalen und ihre Anwendung. PhD Thesis, MPI für Polymerforschung and Universität Mainz; 2001, published at http://archimed.uni-mainz.de/pub/2001/0074.

[45] Torrie GM, Valleau JP. Chem Phys Lett 1974;28(4):578.

[46] Torrie GM, Valleau JP. J Comput Phys 1977;23(2):187.

[47] Beutler TC, Van Gunsteren WF. J Chem Phys 1994;100(2):1492.

[48] Roux B. Comput Phys Commun 1995;91(1–3):275.

[49] Bartels C, Karplus M. J Comput Chem 1997;18(12):1450.

[50] Faller R, Yan Q, de Pablo JJ. J Chem Phys 2002;116(13):5419.

[51] Wang F, Landau DP. Phys Rev Lett 2001;86(10):2050.

[52] Wang F, Landau DP. Phys Rev E 2001;64(5):056101.

[53] Calvo F. Mol Phys 2002;100(21):3421.

[54] Yan Q, Faller R, de Pablo JJ. J Chem Phys 2002;116(20):8745.

[55] Faller R, de Pablo JJ. J Chem Phys 2003;119(8):4405.

[56] Shell MS, Debenedetti PG, Panagiotopoulos AZ. J Chem Phys 2003; 119(18):9406.

[57] Troyer M, Wessel S, Alet F. Phys Rev Lett 2003;90(12):120201.

[58] Yan Q, de Pablo JJ. Phys Rev Lett 2003;90(3):035701.

[59] Sun Q, Faller R. Automatic mapping of polymer mixtures: polyisoprene and polystyrene, in preparation.

[60] Ahlrichs P, Dünweg B. J Chem Phys 1999;111(17):8225.